Molecular desorption of stainless steel vacuum chambers irradiated with 4.2 MeV/u lead ions

E. Mahner, J. Hansen, J.-M. Laurent, and N. Madsen
CERN, 1211 Geneva 23, Switzerland
(Received 5 November 2002; published 16 January 2003)

In preparation for the heavy ion program of the Large Hadron Collider at CERN, accumulation and cooling tests with lead ion beams have been performed in the Low Energy Antiproton Ring. These tests have revealed that due to the unexpected large outgassing of the vacuum system, the dynamic pressure of the ring could not be maintained low enough to reach the required beam intensities. To determine the actions necessary to lower the dynamic pressure rise, an experimental program has been initiated for measuring the molecular desorption yields of stainless steel vacuum chambers by the impact of 4.2 MeV/u lead ions with the charge states +27 and +53. The test chambers were exposed either at grazing or at perpendicular incidence. Different surface treatments (glow discharges, nonevaporable getter coating) are reported in terms of the molecular desorption yields for H_2, CH_4, CO, Ar, and CO_2. Unexpected large values of molecular yields per incident ion up to 2×10^4 molecules/ion have been observed. The reduction of the ion-induced desorption yield due to continuous bombardment with lead ions (beam cleaning) has been investigated for five different stainless steel vacuum chambers. The implications of these results for the vacuum system of the future Low Energy Ion Ring and possible remedies to reduce the vacuum degradation are discussed.

DOI: 10.1103/PhysRevSTAB.6.013201 PACS numbers: 07.30.Kf

I. INTRODUCTION

In preparation of the heavy ion physics with the Large Hadron Collider (LHC) at CERN [1], the former Low Energy Antiproton Ring (LEAR) will be converted to a Low Energy Ion Ring (LEIR) for ion accumulation in LHC. During LEAR studies in 1997 it was measured that the intensity obtained and the stacking time were both a factor of 2 below the LHC requirements [2]. The static LEAR vacuum pressure was about 5×10^{-12} Torr, but local pressure bumps up to 10^{-9} Torr occurred during continuous injection of about 10^8 ions/s. A dynamic pressure increase by a factor of 5 (2.5×10^{-11} Torr) was attributed to the outgassing of vacuum equipment due to the impact of lost lead ions. This effect increased with beam intensity and limited the maximal intensity.

An intensive experimental program on ion-induced gas desorption and its dependence on the surface preparation of stainless steel vacuum chambers was started in 2001 at the CERN Heavy Ion Accelerator (LINAC 3) [3,4], aiming to understand the LEAR vacuum degradation observed in 1997 and to prepare the injector chain for operation with heavy ions under LHC-type conditions.

II. EXPERIMENT

A. Experimental system

An overview of the accelerator used for the measurements is shown in Fig. 1. LINAC 3 delivers shots of $\sim 10^{10}$ Pb^{27+} ions with a length of 560 μs. The shots can be delivered either continuously with a repetition rate of 1.2 s or on request (single shot) using a PS-Booster cycle for triggering. For LEIR purposes the main interest is Pb^{53+}, and to obtain Pb^{53+} the Pb^{27+} ions are sent through a ~ 1 μm thick carbon foil. The stripping process results in pulses of $\sim 1.5 \times 10^9$ Pb^{53+} ions. Figure 1 also shows that after the stripping foil a few magnetic elements are positioned. The three quadrupoles are used for controlling the beam size and divergence in the test chamber. After the quadrupoles a dipole magnet bends the beam towards the experiment and serves to spatially separate the different charge states emanating from the stripping process. A collimator is used to select the desired charge state to be injected into the test chamber.

Figure 2 shows a more detailed drawing of the experimental setup which has been connected to LINAC 3 after the collimator. A sector valve separates the accelerator from the experimental setup such that the test chamber may be changed without disturbing the linac. After the sector valve a long narrow chamber (⌀ 35 mm, $\ell =$ 1100 mm) has been installed, which serves two purposes. First, it separates the high pressure ($\sim 10^{-9}$ Torr) of LINAC 3 from the experiment. Second, as the test chamber is pumped through this conductance, it serves to give a known pumping speed during the experiments. A turbomolecular pumping (TMP) group is used for evacuation from atmospheric pressure, then the test chamber is pumped via the 26.8 ℓ/s conductance (for H_2) by a 400 ℓ/s sputter ion pump (SIP) and a 1200 ℓ/s Ti sublimation pump (TSP). Pressure measurements are made with a Bayard-Alpert gauge (BAG) and a quadrupole residual gas analyzer (RGA), both calibrated. The RGA can be calibrated *in situ* via a gas injection valve. Right before the test chamber a beam position monitor (BPM), which contains an Al_2O_3 fluorescent screen, is used for

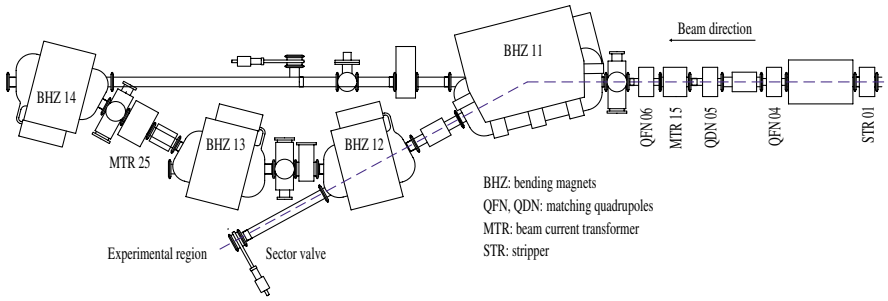

FIG. 1. (Color) Layout of magnetic elements in the LINAC 3 filter line used to steer the ion beam into the experimental setup which is separated by a sector valve from the linac.

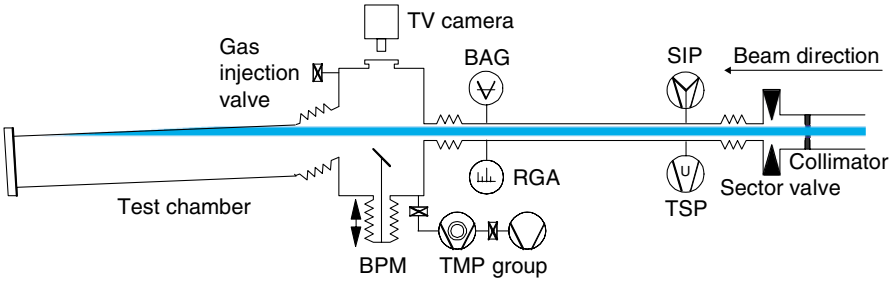

FIG. 2. (Color) The experiment which has been attached at the CERN Heavy Ion Accelerator (LINAC 3) for ion-induced desorption measurements at 4.2 MeV/u.

aligning the ion beam into the test chamber. A TV camera, used for beam observation and alignment, the pumping group, and the gas dozing valve are mounted on the same vacuum chamber in front of the test chamber. The test chamber itself is a 1.4 m long stainless steel tube which can be tilted. The beam line parameters have been calculated, resulting in a 7.7 mm beam size at the entry and ~9.5 mm beam size at the end of the test chamber. The whole experimental line has been aligned with respect to the bending magnets BHZ 11 and BHZ 12 (see Fig. 1).

B. Test chamber preparation

1. Stainless steel chamber A

The 1.4 m long, 145 mm inner diameter vacuum chamber was manufactured from 316LN stainless steel. It was chemically cleaned, first by degreasing at 50 °C with ultrasonic agitation, followed by rinsing in cold demineralized water, rinsing with alcohol, and finally drying with hot air at 80 °C. As an additional treatment, the chamber was vacuum fired for 2 h at 950 °C to reduce the hydrogen content of the bulk material [5] and afterwards baked *in situ* at 300 °C for 24 h after installation. The procedure described above represents the standard CERN treatment which had also been used for the LEAR machine.

2. Glow-discharged chambers B, D, G

Since the gas desorption is stimulated by the impact of energetic heavy ions, a cleaning effect may be achieved by an intense bombardment with ions in a glow discharge. This glow-discharge technique, which has been successfully applied at the CERN Intersection Storage Rings [6], has been used prior to installation of the test chambers in the experimental setup. Three different vacuum chambers (B, D, G) were *ex situ* glow discharged after vacuum firing. Details about the laboratory setup used in this study and the followed glow-discharge procedure can be found elsewhere [7]. A review of glow-discharge techniques for conditioning high-vacuum systems can be also found in the literature [8].

After initial cleaning and vacuum firing like chamber A, chamber B was baked for 24 h at 300 °C, and thereafter exposed to an Ar-O_2 (Ar 90%, O_2 10%) glow discharge with 0.8 A for 1.5 h at 300 °C. This resulted in a total dose of 1.5×10^{18} ions/cm^2. Then, the chamber was baked at 350 °C for 24 h to remove Ar implanted in the stainless steel surface. The chamber was afterwards vented with N_2 before being installed in the LINAC 3 test stand. Finally, test chamber B was baked *in situ* to 350 °C for 24 h.

The chambers D and G, cleaned and vacuum fired in the same way as mentioned above, were also baked in the laboratory setup at 300 °C for 24 h and then immediately glow discharged. For chamber D, again Ar-O_2 was used as discharge gas, the total dose was 3.5×10^{18} ions/cm^2. In

order to investigate a potential influence of the used discharge gas, chamber G was treated with He-O_2 (He 90%, O_2 10%) up to a total dose of 5×10^{18} ions/cm^2. After the glow-discharge treatment was stopped, both vacuum chambers were baked at 350 °C for 24 h, vented with N_2, installed in the experimental setup, and finally baked again *in situ* to 350 °C for 24 h. It should be explicitly mentioned that the glow-discharge treatments of all three vacuum chambers were done at 300 °C.

3. NEG sputter-coated chamber C

There are only a few high energy (MeV/u) measurements of ion or electron desorption yields published for uncoated stainless steel vacuum chambers [9,10], but no data are available for sputter-coated stainless steel. Therefore, it is very interesting to investigate the ion-induced desorption of nonevaporable getter (NEG) films like TiZrV. In the context of the fastidious LEIR vacuum system, this type of film could transform a classical stainless steel vacuum chamber from a "source of gas" into a pump.

After initial cleaning and vacuum firing similar to all other vacuum chambers tested in this study, chamber C was NEG coated with a ~1.5 μm thick film of Ti 30%, Zr 20%, and V 50%. The characteristics of these types of films were studied in great detail at CERN. A description of the vacuum properties and the deposition technique can be found elsewhere [11,12].

After installation in the experimental setup, the chamber was baked to 100 °C for 36 h during which the rest of the system was baked at 300 °C. Next, the temperature was increased by 20 °C/h to 200 °C and left at 200 °C for 24 h in order to activate the NEG coating, while the rest of the vacuum system remained at 300 °C [13]. After first desorption tests, the NEG-coated chamber C was vented with N_2, dismantled, and stored for seven months under vacuum in the laboratory. For a second series of tests the vacuum chamber was reinstalled and baked out a second time, but now, the temperature was increased from 100 °C by 20 °C/h to 300 °C and baked together with the rest of the vacuum system for 24 h.

4. End flanges of the test chambers

For all vacuum chambers tested, the assembled end flanges (perpendicular incidence of the ion beam) were prepared, i.e., cleaned, vacuum fired at 950 °C, Ar-O_2 or He-O_2 glow discharged, NEG coated, and *in situ* baked, exactly in the same way as the corresponding vacuum chamber.

III. EXPERIMENTAL RESULTS

The test chambers have been exposed to lead ion beam impact of Pb^{53+} and Pb^{27+} (only single shots of 1×10^{10} ions), for Pb^{53+} both with continuous injection every 1.2 s as well as single-shot measurements. For the single-shot measurements the pressure development was monitored using the residual gas analyzer with an integration time setting of $\tau = 250$ μs. As will be shown in the results, this speed was necessary to avoid the electronics of the RGA to integrate too much and thereby distort the resulting pressure measurement. Three impact angles θ[1] were investigated: grazing incidence with 89.2° and 84.8° and perpendicular impact ($\theta = 0°$) onto the end flange of the test chamber.

A. Settings of the residual gas analyzer

The electronics of the RGA integrates the ion current signal in order to reduce noise. Partial pressure measurements were carried out where the time scale of relevance could be as small as 10 ms. Therefore, a number of partial pressure measurements were carried out for different settings of the RGA speed.

Figure 3 shows the result of a series of measurements of the ion current development versus time after a Pb^{53+} shot for various settings of the RGA integration time. The measurements lead to the use of a setting of 250 μs as the standard setting for this kind of measurement, as one observes that the change between 25 and 250 μs is negligible. The integration time of the electronics is thus shorter than the time scale of the pressure development.

To extract the molecular desorption yield from measurements as the above, the ideal gas law may be used. The ideal gas law is a law for a gas in equilibrium. Equilibrium in this context means that the changes in the gas occur on a time scale much longer than the mean molecular transit time in the vacuum system. The heaviest molecule studied is CO_2, which at 300 K has a thermal velocity of ~240 m/s. The length of our system is about 2 m, which gives maximum transit times of the order of 10 ms. Care should therefore be taken in drawing conclusions from changes occurring faster than the molecular transit time. It is however interesting to observe that the 10 ms calculated above is about the rise time of the partial pressure of CO. The shot length of 560 μs is furthermore short compared to the other time scales and can thus be ignored in this regard.

B. Equilibrium measurements

In LEAR, ions were lost quasicontinuously; thus one investigation to carry out on the various chambers and with various impact angles is to measure the change in the equilibrium pressure in the test chamber when exposed to continuous bombardment of lead ions. The effective ion-induced desorption yield η_{eff} (molecules/ion) is then given by the conductance method, i.e.:

$$\eta_{\mathrm{eff}} = \frac{\Delta P \times S}{\dot{N}_{\mathrm{Pb}} \times k_B \times T} = G \times \frac{\Delta P \times \mathrm{S}}{\dot{N}_{\mathrm{Pb}}},$$

[1]The impact angle θ is defined with respect to the surface normal of the sample.

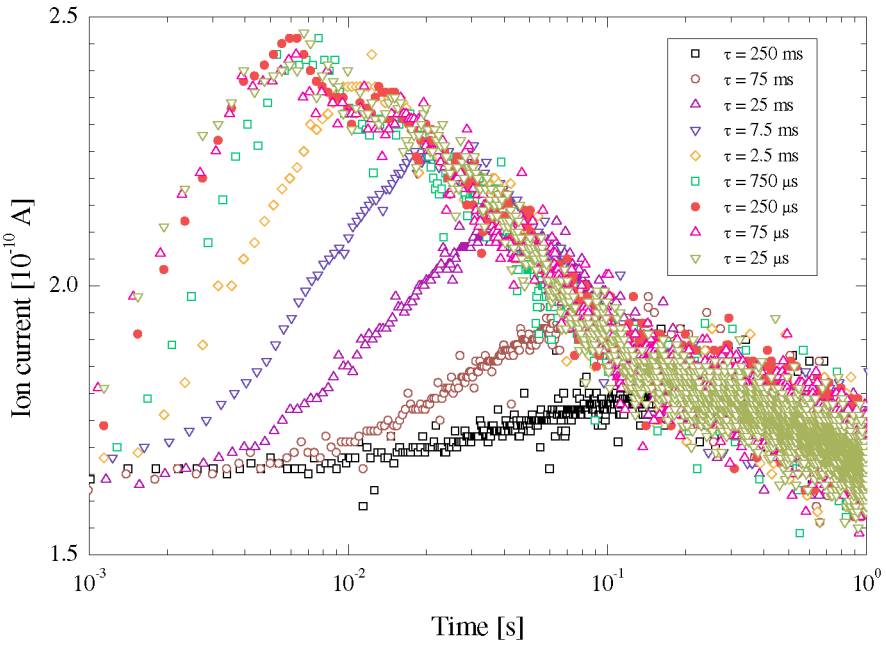

FIG. 3. (Color) Measurement of the development of $m/e = 28$ peak with the residual gas analyzer as a function of time after impact of a shot of Pb^{53+} when chamber A was exposed to repeated pulses every 1.2 s. The inset gives the RGA setting (integration time of the electronics) for the various measurements.

where ΔP is the partial pressure increase in the test chamber under ion bombardment, S is the pumping speed in ℓ/s (for each gas), $\dot{N}_{Pb}$ is the number of impacting lead ions per second, k_B is the Boltzmann constant, T is the temperature (300 K), and G is a constant that converts gas quantities (Torr $\times$ ℓ) into number of molecules ($\approx 3.2 \times 10^{19}$ at 300 K).

Figure 4 shows an example of a measurement of the total pressure in chamber A under various experimental conditions including continuous bombardment with lead ions. From these measurements one finds that the loss of about 1.25×10^9 Pb^{53+} ions/s causes a pressure increase of a factor of 91. With the calculated pumping speed of $S = 26.8$ ℓ/s (for H_2) this results in an effective desorption yield η_{eff} of 2×10^4 molecules per incident Pb^{53+} ion. The reported pressure increase in LEAR was a factor of 5 for a loss rate of about 5×10^7 ions lost per second [2], from which a desorption yield of about 7×10^4 molecules per incident Pb^{54+} can be estimated.

A factor of 3–4 difference is thus observed between the experiment reported here and the LEAR situation in 1997. The ion-induced desorption yield, measured at LINAC 3, confirms that the pressure increase observed in LEAR was due to lost lead ions impacting on the stainless steel vacuum chambers. It has been calculated that the lost ions impact mainly with grazing incidence. However theory and experiments [9] indicate that less grazing incidence (or even perpendicular impact) give smaller desorption yields. Measurements of the yield with 89.2° and 84.8° grazing incidence and perpendicular impact were therefore also carried out.

The cleaning effect evident during the repeated shots (see Fig. 4) has not been observed in LEAR. However, the intensity per unit area on the surface in LEAR was about a factor of 100 smaller, thus careful investigations would have been necessary to observe this.

The maximum equilibrium pressure (P_{max}) under continuous Pb^{53+} bombardment has been measured for three angles ($\theta = 0°$, 84.8°, 89.2°) and for all vacuum chambers, except the glow-discharged chambers D and G that were investigated at $\theta = 89.2°$ only. The results, summarized in Table I, support the earlier assumption that grazing incidence of 89.2° desorbs the most molecules from the surface. In all measurements, the smallest relative pressure rises, defined as the ratio of P_{max} and P_0 (base pressure without beam), were found under perpendicular impact ($\theta = 0°$) onto the end flanges.

A surprise is that the two Ar-O_2 and the He-O_2 glow-discharged chambers are not better than the standard chamber A, rather significantly larger equilibrium pressures were observed in all three chambers at 89.2° grazing incidence. The smallest relative pressure rise was measured for the NEG sputter-coated chamber C, which gave approximately 2 orders of magnitude smaller pressure increase during continuous Pb^{53+} bombardment under 89.2°. It is also observed that the base pressure in the NEG-coated chamber C, measured with

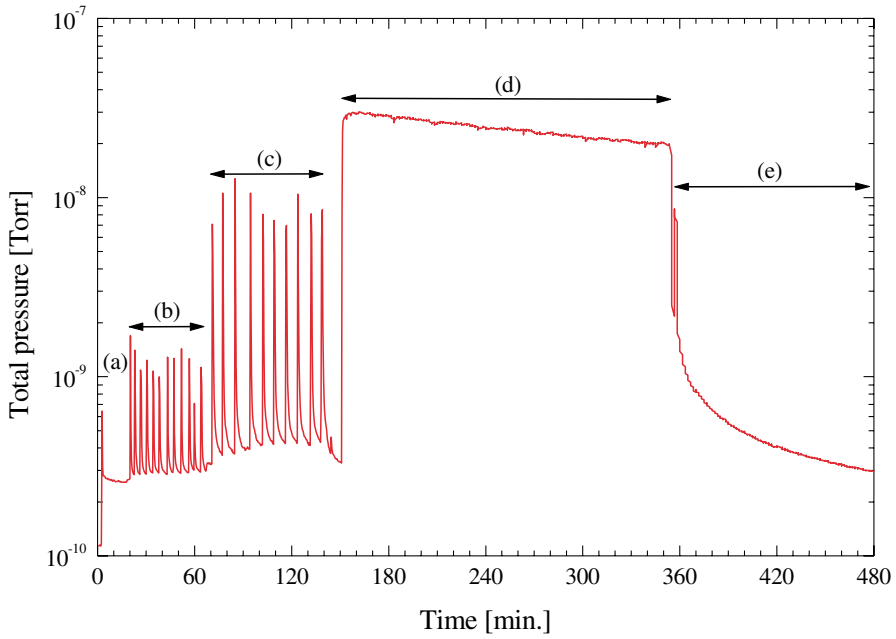

FIG. 4. (Color) Pressure in test chamber A during a period in the experiment. The particles impacted with 89.2° grazing incidence. (a) The sector valve separating the experimental line from LINAC 3 is opened. The pressure in LINAC 3 is higher than the base pressure in the experiment. (b) A series of single shots of 1.5×10^9 Pb^{53+} ions. The time between the shots is the time needed for the vacuum to return to the conditions before each shot. (c) A series of single shots of 1.0×10^{10} Pb^{27+} ions. (d) Pb^{53+} shots are injected with a repetition rate of 1.2 s. (e) The ion beam was switched off, and the pressure decayed. The short pressure increase right after the beam was switched off arose when the sector valve was closed.

TABLE I. Absolute and relative pressure rises in the test chambers when exposed constantly to shots of 1.5×10^9 Pb^{53+} ions every 1.2 s for three different impact angles θ. Normal incidence corresponds to $\theta = 0°$. P_0: base pressure at the beginning of the experiments, measured with open sector valve to LINAC 3. P_{max}: equilibrium pressure under constant ion bombardment.

Vacuum chamber	Charge state q	P_0 (Torr)	P_{max} (Torr) $\theta = 0°$	P_{max} (Torr) $\theta = 84.8°$	P_{max} (Torr) $\theta = 89.2°$
A (no special treatment)	+53	2.5×10^{-10}	3.7×10^{-9} (×15)	1.3×10^{-8} (×42)	2.9×10^{-8} (×91)
B (Ar-O_2 glow discharged)	+53	3.9×10^{-10}	1.3×10^{-8} (×33)	4.3×10^{-8} (×109)	1.5×10^{-7} (×333)
C (NEG, baked at 200 °C)	+53	8.0×10^{-11}	4.0×10^{-10} (×5)	4.0×10^{-10} (×5)	1.3×10^{-9} (×16)
C (NEG, baked at 300 °C)	+53	7.1×10^{-11}	···	···	4.0×10^{-10} (×6)
D (Ar-O_2 glow discharged)	+53	2.4×10^{-10}	···	···	1.4×10^{-7} (×583)
G (He-O_2 glow discharged)	+53	2.6×10^{-10}	···	···	8.3×10^{-8} (×319)

open sector valve (to LINAC 3), is lower than for the other chambers.

C. Single-shot measurements

As described earlier, the operation of LINAC 3 allows to inject single pulses of lead ions into the vacuum chambers under test. This feature allowed us to investigate the dynamic behavior of the desorbed molecules under heavy ion bombardment. To our best knowledge, this technique has never been used before for the study of dynamic effects and the evaluation of effective desorption yields.

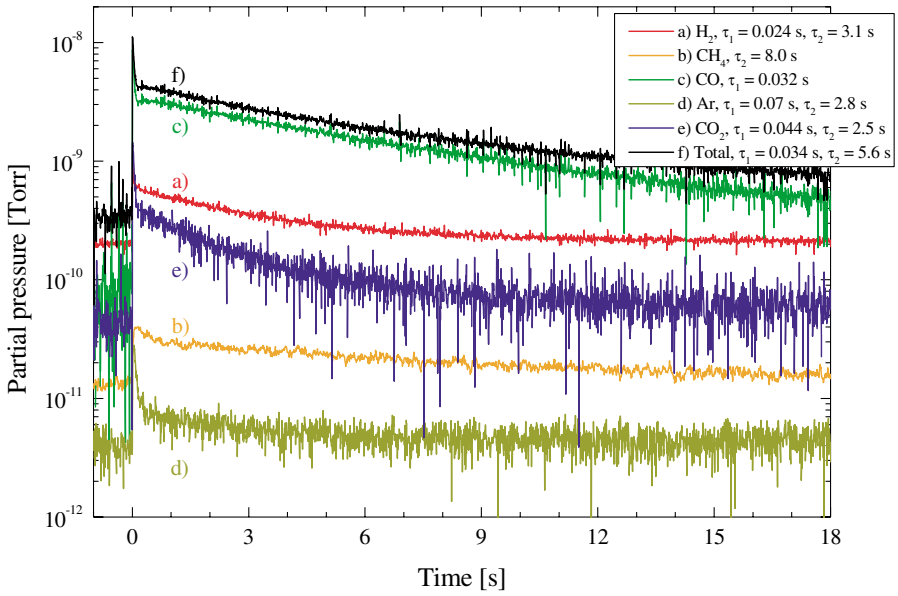

FIG. 5. (Color) Partial pressures measured for chamber A with 1.5×10^9 incident Pb^{53+} ions at 89.2° grazing incidence. The decay times shown in the legend result from two exponential fits to the pressure decays. τ_1 is the result from the fit to the fast part of the decay.

The partial pressures of the major gases, H_2, CH_4, CO, Ar, and CO_2, as a function of time after impact of a single shot of lead ions were measured for both charge states +27 and +53 at each angle. The RGA integration time was set to $\tau = 250\ \mu$s for all these measurements. Figure 5 shows an example of a collection of partial pressure measurements done with chamber A. The RGA can be set to monitor only one m/e peak at a time, thus the partial pressures shown in the figure are calculated assuming that the shots are reproducible. The single-shot reproducibility was tested several times during the experiment and was found to be better than 5%. The individual partial pressures were calculated with the data from an *in situ* RGA calibration.

Several interesting features may be extracted from Fig. 5. The decay of the various partial pressures has been fitted with exponential decays. From these rates an estimate of the pumping speeds of the different gases can be extracted. However, as the fits depend on the exact part of the decay which is fitted, the extracted pumping speeds may be used only as a rough guideline. With a total volume of 76 ℓ, the pumping speeds from the various measurements can be found, assuming that they are limited by the conductance of the ⌀35 mm × 1100 mm tube.

Table II summarizes the pumping speeds derived for H_2, CH_4, CO, Ar, and CO_2. Only the slow part (τ_2) of the pumping (see Fig. 5) has been included in the table. The fast decay observed right after injection has a time scale

TABLE II. Estimated pumping speeds S, tabulated as a function of the ion charge state q and the impact angle θ, extracted from fits to measurements on chamber A. Normal incidence corresponds to $\theta = 0°$. Note that the noise on the argon partial pressure measurement is large compared to the pressure change due to pumping. The pumping speed estimates for argon are therefore very uncertain.

Charge state q	Angle q	S (H_2) (ℓ/s)	S (CH_4) (ℓ/s)	S (CO) (ℓ/s)	S (Ar) (ℓ/s)	S (CO_2) (ℓ/s)
+53	0	23.8	13.1	14.1	11.9	58.5
+53	84.8	23.8	10.1	14.9	⋯	76.0
+53	89.2	24.5	9.5	11.5	27.1	30.4
+27	0	30.4	11.2	15.5	27.1	⋯
+27	84.8	29.9	9.6	14.3	63.3	70.4
+27	89.2	26.2	9.2	10.0	24.5	26.2
Calculated		26.8	9.5	7.2	6.0	5.7

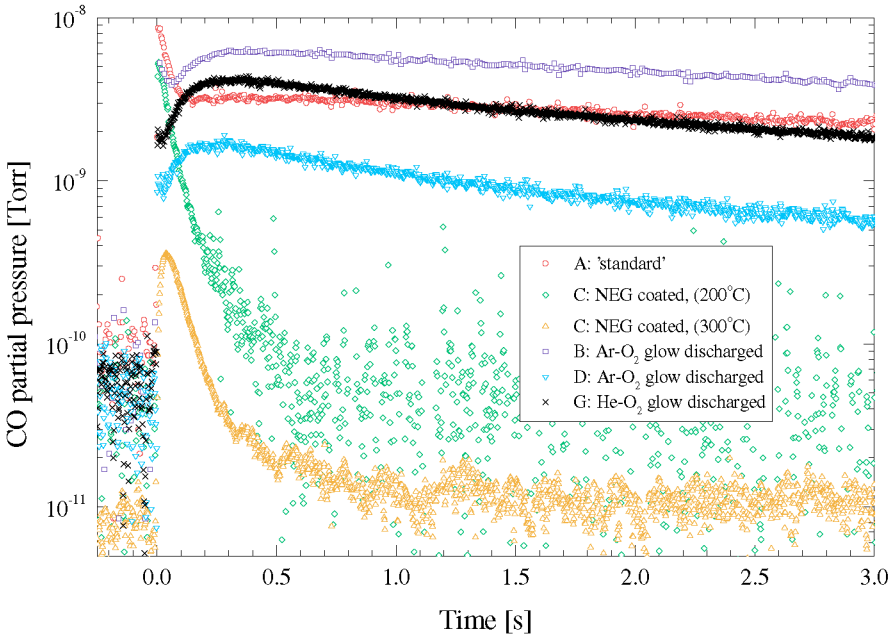

FIG. 6. (Color) CO partial pressure development for five different vacuum chambers measured with pulses of 1.5×10^9 Pb^{53+} ions at 89.2° grazing incidence.

close to the molecular transit times in our system which makes it difficult to quantize. This fast decay was however observed reproducibly for the other tested vacuum chambers. Thus it is believed to represent some physical effect, but we do not presently have enough information to speculate as to the nature of the process behind this observation. The correspondence between the theoretical and the measured pumping speeds given in Table II is quite good, apart from the pumping speeds of Ar and CO_2. As we normally have very little Ar in the chamber this gives an extra twist of uncertainty, and it may be that this pumping is dominated by sticking (readsorption on the surface). CO_2 is usually present in abundance, thus only sticking seems to be responsible for the discrepancy. However, for the low masses the measured decay rates are in good agreement with the calculated values. We therefore conclude that the single-shot measurements are a good means to measure the ion desorption yields. The pumping speeds are however not quite good enough to be used to calculate the effective desorption yield. Nevertheless, another method is possible which will be described now.

D. Effective desorption yields

The next issue to address from these measurements is thus the effective desorption yield. Even though, as may be seen in Fig. 5, pressure changes on time scales of tens of milliseconds were observed, the desorption yield has been calculated from the difference between the peak pressure of the gas in question and the mean pressure right before impact of the lead ions. The effective desorption yields $\eta_{\mathrm{eff,ss}}$, measured with single shots, have been calculated using the ideal gas law[2]

$$\eta_{\mathrm{eff,ss}} = \frac{\Delta P \times V}{N_{\mathrm{Pb}} \times k_B \times T} = G \times \frac{\Delta P \times V}{N_{\mathrm{Pb}}},$$

where ΔP is the partial pressure increase in the test chamber after one shot, V is the test volume ($\approx 76\ \ell$), and N_{Pb} is the number of impacting lead ions. Implicitly this means, it has been assumed, that the number of molecules desorbed is proportional to the number of lead ions. During the experiment the current varied sometimes up to 20%, and no indication of stronger than linear dependency on current was observed. In order to verify this assumption, a dedicated test has been performed with chamber A that was bombarded continuously every 1.2 s with Pb^{53+} ions under 89.2° grazing incidence. The pulse length of the lead ions was decreased from the nominal value of 560 μs (1.4×10^9 ions) in several steps to 200 μs (5×10^8 ions). In that range the number of desorbed molecules was found to decrease linearly with the number of injected lead ions. An example of the CO partial pressure development due to the impact of a single Pb^{53+} shot, measured for all vacuum chambers, is displayed in Fig. 6. The effective desorption yields, measured for 4.2 MeV/u lead ions incident on different stainless steel vacuum chambers, are summarized in Fig. 7 and Table III.

[2]This implies the assumption of zero pumping.

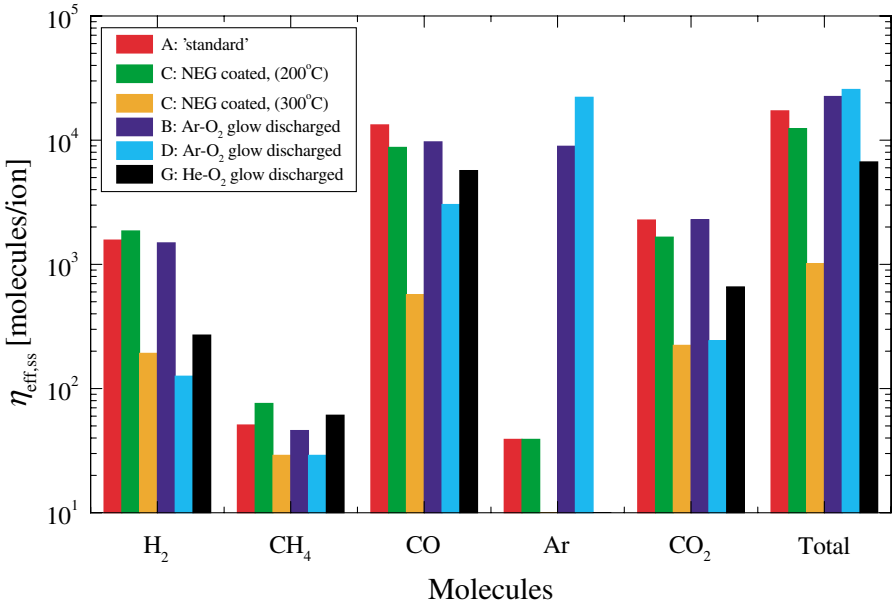

FIG. 7. (Color) Effective desorption yields measured with single shots of 1.5×10^9 Pb^{53+} ions at 89.2° grazing incidence. The yields were calculated using the ideal gas law and the instantaneous pressure increase due to the single shots. Pumping has been ignored in the calculation; the desorption yields for the NEG-coated chamber C are therefore underestimated.

TABLE III. Effective desorption yields of the main desorbed gases measured for 4.2 MeV/u lead ions incident on different stainless steel vacuum chambers. Desorption yields are tabulated as a function of the ion charge state q and the impact angle θ. Normal incidence corresponds to $\theta = 0°$.

			Effective desorption yield $\eta_{eff,ss}$ (molecules/ion)					
Vacuum chamber	Charge state q	Angle θ	H_2	CH_4	CO	Ar	CO_2	Total
A (no special treatment)	+53	0	861	44	7128	14	1805	9852
	+53	84.8	662	31	5382	9	1234	7318
	+53	89.2	1570	51	13 294	39	2276	17 230
	+27	0	92	4	816	2	222	1136
	+27	84.8	135	9	868	2	220	1234
	+27	89.2	557	41	4357	7	613	5575
B (Ar-O_2 glow discharged)	+53	0	888	41	7580	305	1662	10 477
	+53	84.8	1188	42	8108	2161	2053	13 552
	+53	89.2	1493	46	9699	8950	2288	22 476
	+27	0	122	5	927	92	259	1404
	+27	84.8	118	1	2061	851	497	3528
	+27	89.2	239	19	8452	6449	1927	17 086
C (NEG, baked at 200 °C)	+53	0	775	35	4336	11	394	5551
	+53	84.8	845	40	5109	9	368	6371
	+53	89.2	1859	76	8750	39	1656	12 380
	+27	0	169	6	1239	2	92	1507
	+27	84.8	142	7	1109	2	252	1514
	+27	89.2	330	50	1360	4	245	1988
C (NEG, baked at 300 °C)	+53	89.2	192	29	569	···	223	1013
D (Ar-O_2 glow discharged)	+53	89.2	126	29	3039	22 176	243	25 613
	+27	89.2	24	20	939	9881	120	10 984
G (He-O_2 glow discharged)	+53	89.2	270	61	5695	···	658	6684

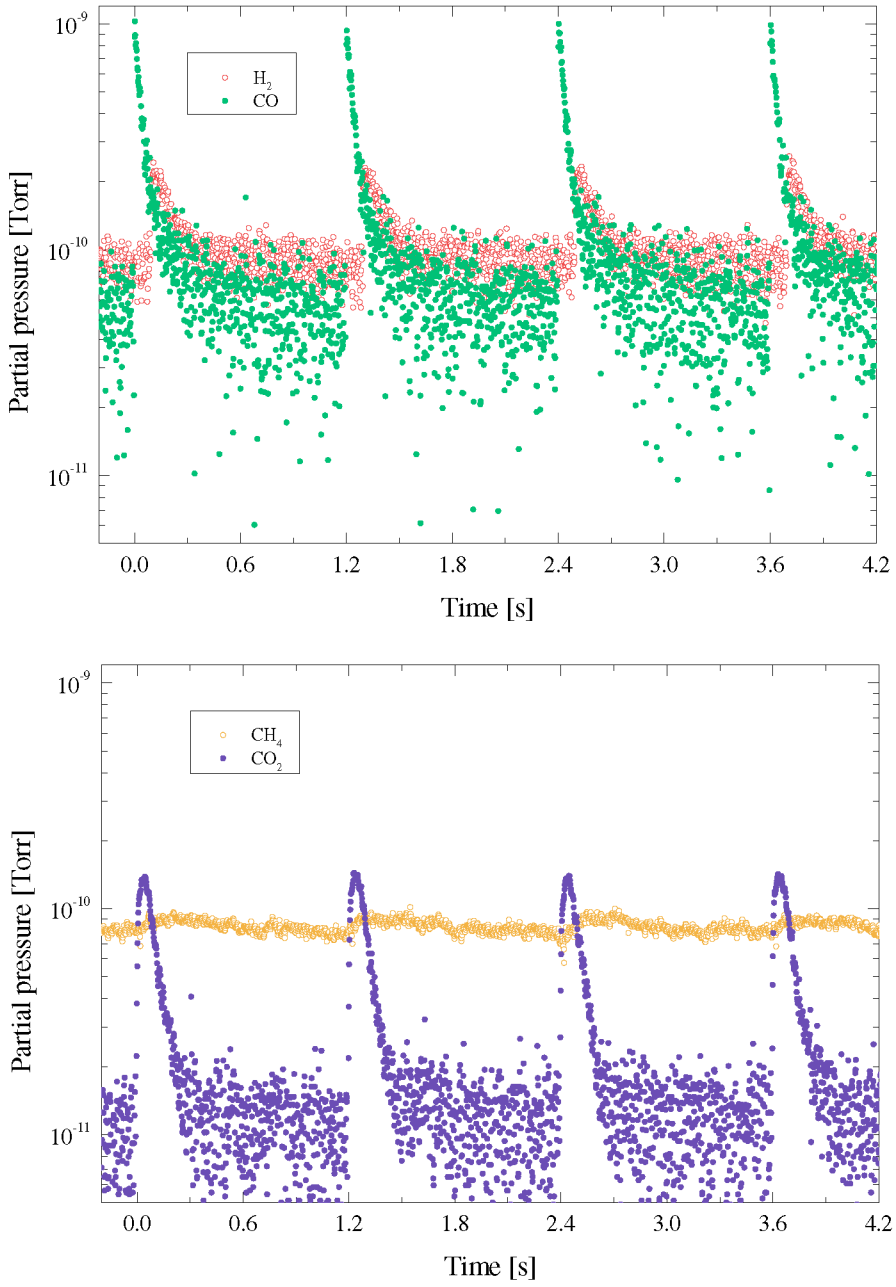

FIG. 8. (Color) Partial pressures measured for the NEG-coated vacuum chamber C (activated at 300 °C) with pulses of 1.5×10^9 Pb^{53+} ions every 1.2 s impacting at 89.2° grazing incidence. Upper curve: H_2 and CO, lower curve: CH_4 and CO_2.

1. Yields for chamber A

For vacuum chamber A, the main component desorbed is CO, independent of the ion charge state and the angle of incidence. It is also evident (from Table III) that grazing incidence of 89.2° has the highest effective desorption yield. The total desorption yield measured with the single-shot method is in agreement with the yield extracted from the equilibrium measurements under exposure of chamber A to ion shots every 1.2 s. We observe that the desorption yield of Pb^{27+} is significantly lower than for Pb^{53+}, the difference being smallest at 89.2° grazing incidence, where it is a factor of 3. The fact that CO is the main molecule desorbed under heavy lead ion bombardment is in agreement with qualitative results obtained at LEAR. In fact this observation was the main reason for the tests of the glow-discharged vacuum chambers B, D, and G, as it has been found earlier that this treatment can remove carbon very efficiently from the surface [14].

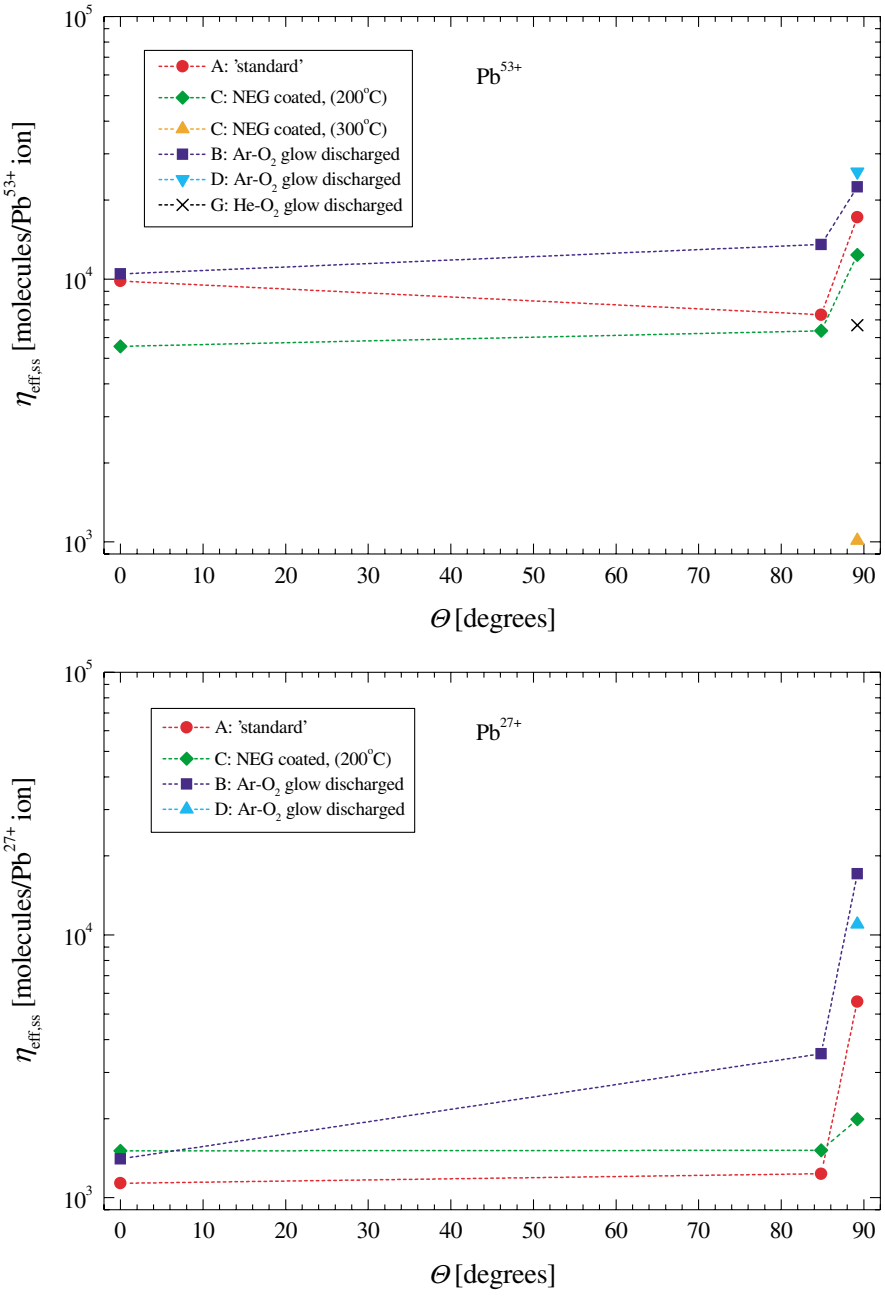

FIG. 9. (Color) Effective desorption yields of lead ions at 4.2 MeV/u measured for three different impact angles θ and two charge states q. Upper curve: Pb^{53+}, lower curve: Pb^{27+}. Normal incidence corresponds to $\theta = 0°$.

2. Yields for chambers B, D, G

From the yields measured for the Ar-O_2 glow-discharged chambers, summarized in Table III, a couple of conclusions may be drawn. First of all, one observes that the total effective desorption yields of chambers B and D have not been reduced as expected, rather they are larger than those of chamber A. For Pb^{53+} bombardment at 89.2° grazing incidence the total yields are 30% to 50% higher than for chamber A, while the difference is largest (a factor of 2 to 3) for Pb^{27+} injection at the same impact angle. The biggest difference can be seen in the obtained Ar yields for chambers B and D, which are enhanced by nearly 3 orders of magnitude. Apparently, the 350 °C bakeouts after the glow-discharge treatment were not sufficient to remove completely the amount of Ar implanted before. This effect is most probably related to the direct impact of the high energy lead ions onto the stainless steel.

The best results for the glow-discharged tubes have been obtained with chamber G, where He has been used

as discharge gas instead of Ar. In that case, no Ar could be detected as a desorbed molecule, but an increased amount of desorbed He was measured with the RGA during continuous bombardment with heavy ions. In comparison with chambers B and D, the total effective desorption yield of G, measured for Pb^{53+} injection at $\theta = 89.2°$, is reduced by a factor of 3.4 to 3.8. For the uncoated stainless steel vacuum chambers tested so far, the He-O_2 glow-discharge treatment gave the smallest ion yields, but there are still $\sim$7000 molecules/Pb^{53+} ions desorbed.

3. Yields for chamber C

The NEG-coated vacuum chamber C gave very interesting results under heavy lead ion bombardment; they are also listed in Table III. After the 200 °C bakeout of the TiZrV getter we observed slightly smaller effective desorption yields than for chamber A, but not with more than a factor of 2 in the best case. As for the other vacuum chambers (except chamber D), the desorption of mass 28 (CO) is strongly enhanced in comparison to the yields obtained for H_2, CH_4, Ar, and CO_2. A further reduction in the measured effective yields was found during a second series of tests, where the NEG-coated chamber had been baked at 300 °C. Not only the η for CO, but also the total effective desorption yield of $\sim$1000 molecules/Pb^{53+} ion was reduced by approximately 1 order of magnitude in comparison with the first test of the getter.

In addition, the pumping speeds might be of interest. For the TiZrV sputter-coated chamber C the pumping speed cannot be measured using the decay rate of the partial pressure of the different gases, as can be done for stainless steel. The reason for this is that the sticking probability on a NEG surface is so high that the pressure measurement carried out in the RGA is not representative for the pressure development inside the vacuum chamber.

The high pumping speed of chamber C was investigated with continuous injection of heavy lead ions every 1.2 s. The obtained results are displayed in Fig. 8. Because of the large pumping speed of the getter film, the initial partial pressures of H_2, CO, and CO_2, measured before ion impact, are reached again before the next shot is injected 1.2 s later. These measurements, that can be directly compared with the results obtained for chamber A (see Fig. 5), confirm the functioning of the NEG. It should be kept in mind that the partial pressures are measured with the RGA which is located $\sim$0.7 m upstream of the entrance of test chamber C. As the pumping speed of the sputter-coated NEG is rather large compared to the time scale of molecular transit, the effective desorption yield measurements, assuming zero pumping, underestimate the actual desorption of the NEG coating.

4. Impact angle and charge state dependence

The effective ion-induced desorption yields have been measured for Pb^{53+} and Pb^{27+} as a function of the impact angle. A summary of the results obtained is displayed in Fig. 9.

From Fig. 9 and Table III it becomes evident that grazing incidence of 89.2° yields more desorbed molecules than less grazing incidence or even perpendicular impact. The difference between the two extremes has been observed to be a factor of 2 for Pb^{53+} ions. We also measured a significant influence on the charge state of the lost ions. This effect is probably linked to the dependence of sputtering on the stopping power, which scales with the charge state [15]. In surface layers where the ion adjusts its charge state to the equilibrium value Z_{eq}, the energy loss and the desorption yield may be larger ($q > Z_{eq}$) or smaller ($q < Z_{eq}$) than at deeper layers ($q = Z_{eq}$).

E. Beam scrubbing

The results described above were all obtained using a ''single-shot technique,'' where a single pulse of lead ions was injected into the test vacuum chamber. This feature allowed us to investigate the dynamic behavior of the desorbed molecules under heavy ion bombardment. For the operation of the LEIR vacuum system the ion-induced desorption due to continuous injection of lead is most important to understand and was studied as well. Therefore, all vacuum chambers have been continuously (every 1.2 s) bombarded with Pb^{53+} ions under 89.2° grazing incidence for up to 200 h at the most. The measured total pressure increase ΔP and the calculated effective desorption yield η_{eff} are displayed in Fig. 10.

It is demonstrated that the standard vacuum chamber A is cleaned by continuous impact of heavy lead ions. The effective desorption yield is decreased by a factor of 10 after the impact of about 2.4×10^{11} ions/cm^2 during 15 h. A factor of 50 is gained after 55 h continuous Pb^{53+} bombardment. An important issue is that after venting with N_2 (for 5 min, no flange was opened), followed by pumping and a new bakeout for 24 h at 300 °C, a part of the beam cleaning is kept. A comparison of how long beam cleaning would take in LEIR in order to gain a factor of 10 is hard to predict because it depends on the total loss area, the effective desorption yield, and the local pumping speed.

The glow-discharged vacuum chambers show a very similar behavior in terms of beam cleaning, therefore, there is no big advantage in applying this technique for the LEIR vacuum chambers. Nevertheless, it could be interesting to investigate a vacuum chamber that will be *in situ* (already attached to LINAC 3) glow discharged and then not vented prior to the ion-induced desorption tests. The smallest relative pressure rise was measured for a NEG sputter-coated vacuum chamber C, activated at 300 °C, which gave approximately 2 orders of magnitude smaller pressure increase during continuous Pb^{53+} bombardment under 89.2°. The same vacuum chamber had been previously activated at a lower temperature (200 °C)

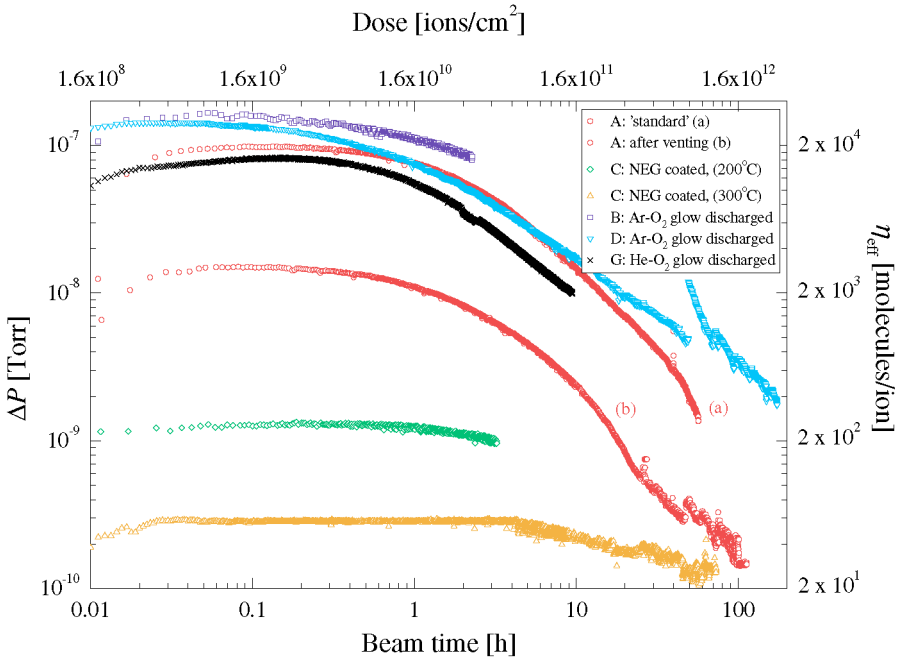

FIG. 10. (Color) Beam cleaning measurements for five different stainless steel vacuum chambers continuously bombarded with 1.5×10^9 Pb^{53+} ions (per shot) under $\theta = 89.2°$ grazing incidence. The results obtained for Ar-O_2 and He-O_2 glow-discharged vacuum chambers and a NEG-coated chamber, activated at 200 °C and 300 °C, are compared with an untreated (''standard'') vacuum chamber [curve (a)]. This chamber was vented after 60 h bombardment (no flange was opened), pumped, baked, and measured again [curve (b)]. The calculated effective desorption yield (right axis) cannot be applied to the NEG-coated chamber C.

resulting in higher effective desorption during continuous bombardment with lead ions. So far, the lowest dynamic pressure was obtained with a standard stainless steel vacuum chamber, sputter coated with a nonevaporable getter film of approximately 1.5 μm thickness, and activated at 300 °C.

IV. CONCLUSIONS AND OUTLOOK

The following list of issues summarizes the results of the experiments carried out so far.

The measurements show that with a loss of about 1.25×10^9 Pb^{53+} ions/s under $\theta = 89.2°$ grazing incidence the equilibrium pressure increases by up to 3 orders of magnitude which results in an effective desorption yield of about 2×10^4 molecules/Pb^{53+} ion.

The estimated desorption yield from the LEAR pressure increase was 7×10^4 molecules per incident Pb^{54+} ion. A factor of 3–4 difference is thus observed between the experiment reported here and the LEAR situation; however the uncertainty on the LEAR estimate is rather large as the pumping speed was not precisely known. We conclude that the cause for the LEAR pressure increase has now been identified with certainty.

The Ar-O_2 and He-O_2 glow-discharge cleaning carried out does not show any signs of having reduced the desorption yields. Furthermore, the chambers exhibit large Ar and He desorption yields indicating that the glow discharge mainly has resulted in argon and helium being implanted into the surface.

The single-shot desorption rate for the NEG-coated chamber, activated at 200 °C for 24 h, did not significantly differ from that of the uncoated stainless steel, but after a 300 °C bakeout the measured total effective desorption was approximately 1 order of magnitude lower than after the first test of the getter.

We observe in all cases that the bulk of the molecules desorbed is CO. CO_2 and H_2 are the second most abundant species in the desorbed gas. CO contributes in fact 70% to 80% of the desorbed molecules. This means that not only the loss of lead ions does cause an increase in pressure, but also a worsening of the vacuum composition.

The results presented in Sec. III E have important consequences for the design of the LEIR vacuum system [16]. The possibility to improve the dynamic pressure by continuous impact of Pb^{53+} ions under grazing incidence has been proven at 4.2 MeV/u. Therefore, one can conclude that ion-induced beam cleaning of the future LEIR vacuum system will be an effective tool to reduce the dynamic pressure in LEIR. During the commissioning of the LEIR vacuum system, sufficient

time should be foreseen to apply this beam-scrubbing technique. Of course, if one could locally increase the pumping speed or reduce the desorption yield where the ions are lost (for example at the end of the bending magnets) the necessary time for beam scrubbing would decrease. This has been verified in the experiments done at LINAC 3. Wherever possible, linear pumping in the form of a nonevaporable getter should be incorporated in the machine design, especially in the bending magnets (conductance limited), but also in the tanks of the injection septa, the ejection kicker, and generally in the short straight sections of LEIR. The choice of getter, either sputter coated or commercially available NEG's, must be carefully evaluated. The positions where the lead ions will be lost must be known precisely (5–10 cm) along the LEIR machine in order to put special absorbers (low outgassing under heavy ion impact) and high local pumping speed. The lost ions should bombard these absorbers preferentially under $\theta = 0°$ (perpendicular impact) to minimize the desorption yields.

For future studies at LINAC 3 some interesting questions remain to be studied. The fundamental problem being faced here might be that the lost lead ions desorb molecules who are embedded deeper into the surface than any of the various surface cleaning methods can penetrate. Therefore, one interesting experiment would be to electropolish and chemically polish the vacuum chambers before vacuum firing at 950 °C to study the possible influence of the damaged surface layer (due to the fabrication of the stainless steel sheets) on the ion-induced desorption. It might be also interesting to study the influence of the stainless steel oxide layer and to compare the desorption of the NEG coating with a commercially available getter.

ACKNOWLEDGMENTS

The experiments described could not have been done without the help and assistance of many people at CERN. First of all, it is a pleasure to thank the PS division, especially K. Schindl and the LINAC 3 team, C. Hill, D. Küchler, M. O'Neil, R. Scrivens, J. Broere, and R. Hajdas, for making the linac available, very reliable, and useful to us. Fruitful suggestions, discussions, and comments from C. Benvenuti, M. Chanel, P. Chiggiato, I. Collins, O. Gröbner, N. Hilleret, D. Möhl, and P. Strubin are appreciated very much. Furthermore, we would like to thank P. Costa Pinto for the NEG coating of chamber C. Finally, we are grateful for the technical support we have received both during setup and running of the experiment from D. Allard, C. Lacroix, K. Magyari, S. Southern, and J. P. Pasquet with his team.

[1] The LHC Study Group, P. Lefevre and T. Pettersson, The Large Hadron Collider, conceptual study, CERN Report No. CERN/AC/95-05 (LHC), 1995.
[2] J. Bosser, C. Carli, M. Chanel, C. Hill, A. Lombardi, R. Maccaferri, S. Maury, D. Möhl, G. Molinari, S. Rossi, E. Tanke, G. Tranquille, and M. Vretenar, Part. Accel. **63**, 171 (1999).
[3] J. Hansen, J.-M. Laurent, N. Madsen, and E. Mahner, CERN Report No. LHC/VAC-TN-2001-07, 2001.
[4] M. Chanel, J. Hansen, J.-M. Laurent, N. Madsen, and E. Mahner, in *Proceedings of the IEEE Particle Accelerator Conference, Chicago, IL, 2001* (CERN Report No. PS-2001-040-AE, 2001).
[5] R. Calder and G. Lewin, Br. J. Appl. Phys. **18**, 1459 (1967).
[6] R. Calder, Vacuum **24**, 437 (1974).
[7] A. G. Mathewson, CERN Report No. CERN-LEP-VA/87-63, 1987; CERN Report No. CERN-ISR-VA/76-5, 1976; R. Calder, A. Grillot, F. Le Normand, and A. Mathewson, CERN Report No. CERN-ISR-VA/77-59, 1977; in *Proceedings of the 7th International Vacuum Congress and the 3rd International Conference on Solid Surfaces*, edited by R. Dobrozemsky, F. Rüdenaver, F. P. Viehböck, and A. Breth (F. Berger & Söhne, Vienna, 1977), Vol. I, p. 341.
[8] H. F. Dylla, J. Vac. Sci. Technol. A **6**, 1276 (1988).
[9] S. Y. Zhang and L. A. Ahrens, in *Proceedings of the 1999 Particle Accelerator Conference, New York, 1999* (IEEE, Piscataway, NJ, 1999), p. 3294.
[10] P. Thierberger, A. L. Hanson , D. B. Steski, V. Zajic, S. Y. Zhang, and H. Ludewig, Phys. Rev. A **61**, 042901 (2000).
[11] C. Benvenuti, J. M. Cazeneuve, P. Chiggiato, F. Cicoira, A. Escudeiro Santana, V. Johanek, V. Ruzinov, and J. Fraxedas, Vacuum **53**, 219 (1999).
[12] C. Benvenuti, P. Chiggiato, A. Mongelluzzo, A. Prodromides, V. Ruzinov, C. Scheuerlein, M. Taborelli, and F. Levy, J. Vac. Sci. Technol. A **19**, 2925 (2001).
[13] P. Chiggiato (private communication).
[14] A. G. Mathewson, Vacuum **24**, 505 (1974).
[15] M. Toulemonde, W. Assmann, C. Trautmann, and F. Grüner, Phys. Rev. Lett. **88**, 057602 (2002); C. Trautmann (private communication).
[16] E. Mahner, CERN Report No. LHC/VAC-TN-2002-04, 2002.